OPTOELECTRONICS AND ADVANCED MATERIALS – RAPID COMMUNICATIONS Vol. 2, No. 10, October 2008, p. 603 - 613

3D numerical noise modeling and simulation of a MISFET photodetector in the nanometer region

K. BALASUBADRA[a], V. RAJAMANI[b*], K. SANKARANARAYANAN[c]
Department of Electronics and Communication Engineering
[a]K.L.N.College of Information Techn., Sivagangai, TN, India - 630 611
[b]PSNA College of Engg. and Tech., Dindigul, TN, India - 624 622
[c]V.L.B. Janakiammal Engg. College, Coimbatore, TN, India - 641 042.

A 3D numerical noise model has been developed for computation of different noises in metal-insulator-semiconductor field effect transistor (MISFET) in the nano meter region. Two port small signal noise equivalent model has been developed to study the overall noise performance. Shot noise, thermal noise and diffusion noise components have also been calculated for the two port MISFET photodetector. Signal-to-noise ratios (SNR), BER and Noise Equivalent Power (NEP) have also been calculated. The operating frequency can be adjusted suitably to make the noise behavior of the MISFET independent of the value of the incident optical power.

(Received January 24, 2008; accepted August 14, 2008)

Keywords: 3D Noise modeling**,** Two port small signal noise model, MISFET photodetector, Signal-to-noise ratio (SNR), Noise equivalent power (NEP), Bit error rate (BER).

1. Introduction

The development of integrated circuit (IC) technology over the past several decades has had a profound impact on society, paving the way to the information revolution. The extra ordinary advances in semiconductor technology in the fast few decades have resulted in the mass production of semiconductor devices having characteristics length below 1µm.The driving forces for the IC revolution and technological innovations are miniaturization and manufacturing micro or nano system architectures. Over the last few decades, the minimum feature size of the IC device has scaled down by forty fold and the functional density of chips has increased from dozens of transistors to the billions of transistors. Technology scaling in modern day VLSI has resulted in an exponential growth in the transistor performance at the sacrifice of both dynamic as well as static power. However, technology scaling reaps the high benefits of oxide thickness scaling and length scaling. The reason for this is that the numerical approach is readily available to any 3D problems such as short channel effect or narrow width effect, while it is almost impossible to deal analytically with such problems without resorting to some sort of assumptions or approximations. Therefore it is worthwhile to realize a device using a numerical device model to make full use of the numerical model's accuracy in simulation.

To attain much higher performances of both FET's and circuits, it is of great importance to scale down device sizes, especially gate length-without undesirable short channel effects. Among the CMOS family of FETs, Metal Insulator Semiconductor Field Effect Transistors (MISFET), is chosen due to its flat impedance over a large frequency range, simplifying impedance matching for wide band amplifiers, high current drivability, large noise margin, high breakdown voltage, high channel aspect ratio, low gate leakage and high breakdown voltage for higher power density and Compatible accumulation and depletion mode devices.

With the advent of technology of III-V semiconductors it has become possible to develop MISFET structures based on compound semiconductors [1]. Quite a large number of MISFET structures based on III – V semiconductors have been proposed, fabricated and tested for various applications including photodetection [2,5]. In recent years, the low noise MISFET photodetectors have drawn considerable attention for use in optical receivers due to its integrated circuit compatibility.

Yamaguchi and Kobayashi [2] demonstrated the operation of an enhancement mode MISFET as a new high gain photodetector. The light was focused on the semi-transparent metal gate to increase the photosensitivity. It was shown that the photocurrent gain in the order of 10^3 can be obtained under application of gate bias. It was explained that the amplification is due to the increase in the surface channel conductivity via the development of an electron quasi-Fermi level shift towards the conductive-band edge under illumination.

The physics based theoretical models were developed by Chakrabarti *et al* [3,4] to examine the optically controlled characteristics of a heterogate MISFET structure and reported that the device characteristics significantly influenced by incident radiation. These models were developed based on one dimensional analysis

considering constant and field independent mobility of the carriers in the surface channel. K. Ohata [5] explained that InP is a promising semiconductor for the fabrication of FET's for microwave high-power applications because of its reduced trapping and thus of its lower noise over other materials .

Photoresponse characteristics of a three dimensional numerical model of nano MISFET photodetector was presented for suitability in the OEIC receiver application [6]. The effect of various internal device parameters such as electric filed, mobility of the carriers in the presesnce of illumination, potential distribution of the carriers have also been studied extensively through numerical simulation.

Asgaran and Jamaldeen [7] made simple closed form expressions for MOSFET's noise parameters and were developed and verified. The expressions were explicit functions of MOSFET geometry and biasing conditions, hence making them useful for circuit design purposes and to be incorporated in simulators such as SPICE. Moreover, It was demonstrated that the effect of induced gate noise on the accuracy of noise models was negligible. Nanua and Blaauw[8] demonstrated the effects of the noise injection, noise propagation and noise failure in the MOSFET. In SOI, the threshold voltage variation would cause significant variation in the amount of propagated noise and injected noise. It is dealt with the calculation of specific body voltages during noise analysis.

A l/f noise model based on the distributed equivalent circuit technique for evaluating the semi-insulating substrate is proposed by K.T. Yan and Forbes [9]. It was shown that the l/f noise is a bulk phenomena with localized high frequency variations and long range low frequency fluctuations with the lowest frequency being constrained by the thickness of the material. Signal and noise modeling of dual-gate MESFET is presented by Olivera and Vera Markovie [10]. A set of equations describing the noise parameters of each single-gate MESFET as the function of three equivalent noise wave temperatures is implemented within the circuit simulator Libra. A general CAD procedure is developed for the signal and noise parameters extraction of complete dual-gate MESFET.

The procedure for defining two noise models of MESFET, HEMT transistors as new elements of standard microwave circuit simulator Libra is described by Natasa et al. [11]. The first implemented model is based on equivalent temperatures including complete correlation between intrinsic transistor noise sources, while the second model extends the first one by involving the gate-leakage current influence. Chih-Hung chen and Jamaldeen [12] proposed a new channel noise model using the channel length modulation (CLM) effect to calculate the channel noise of deep submicron MOSFETs**.** The noise contributions from the velocity saturation region and from the hot electron effect seem to be negligible in the channel noise modeling of deep submicron MOSFETs.

It was observed by Z.Celik [13] that Random Telegraph Signal is a major obstacle in modeling low-frequency noise in advanced MOSFETs due to the lack of data and understanding about the different species of traps responsible for RTS and not being able to include quantum effects in the models. Jonghwan Lee et al. [14] presented a physical and analytical model describing the gate-leakage current noise in ultrathin gate oxide MOSFETs, is suitable for implementation in circuit simulators. The model is based on the barrier height fluctuation model and the Lorentzian-modulated shot noise model of the gate-leakage current. Matthias Rudolph et al presented an algorithm that allows for extraction of the noise parameters directly from NF measurements [15]. Gholamreza Moradi and Abdipour [16] introduced a simple algorithm for extracting the input and output equivalent noise temperatures of FET devices. The variation in noise parameter with respect to gate width and the variation of noise temperatures with bias current have been studied.

In present analysis, the various noise components such as shot noise, diffusion noise, thermal noise and the correlation noise of the MISFET photodetector is investigated numerically. The signal-to-noise ratio and the bit error rate have also been computed numerically.

2. Noise modeling

The device under consideration is an optically controlled MISFET. It is similar to a conventional MISFET except for the fact that the former uses a semi-transparent metal gate to facilitate the transmission of the incident radiation inside the device as shown in Fig.1. The light was focused on the semi transparent metal gate to increase the photosensitivity. Application of a large positive voltage on the metal gate causes a strong inversion to occur in the semiconductor at the interface. When an optical radiation of suitable wavelength is incident on the surface of the semi transparent metal gate, a part of the total incident optical power is transmitted through the insulation layer into the semiconductor where it is absorbed. Absorption of this radiation results in the generation of excess electron-hole pairs and the photocurrent is obtained in the order of 10^{3}.

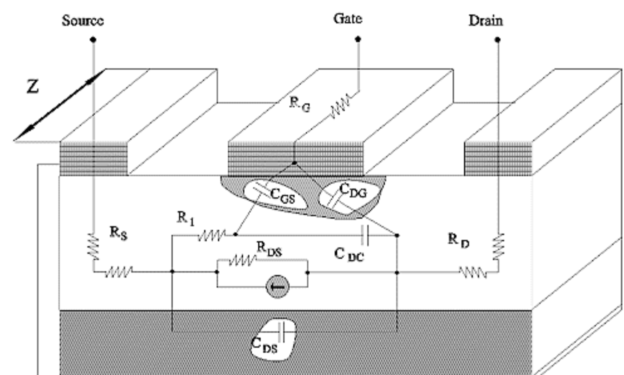

Fig 1. Schematic of the MISFET showing the various components.

The major noise components of MISFET photodetector are 1. gate and drain diffusion noise, 2. gate and drain shot noise and 3. thermal noise arising from various resistances. The first two components are strongly influenced by the incident radiation.

The small signal model of the MISFET photodetector is shown in Fig. 2. In deriving the noise equivalent circuit, we have neglected R_1, R_s, and R_d of the MISFET equivalent circuit as shown in the Fig. 1. These values are negligibly small for the practical MISFET photodetector.

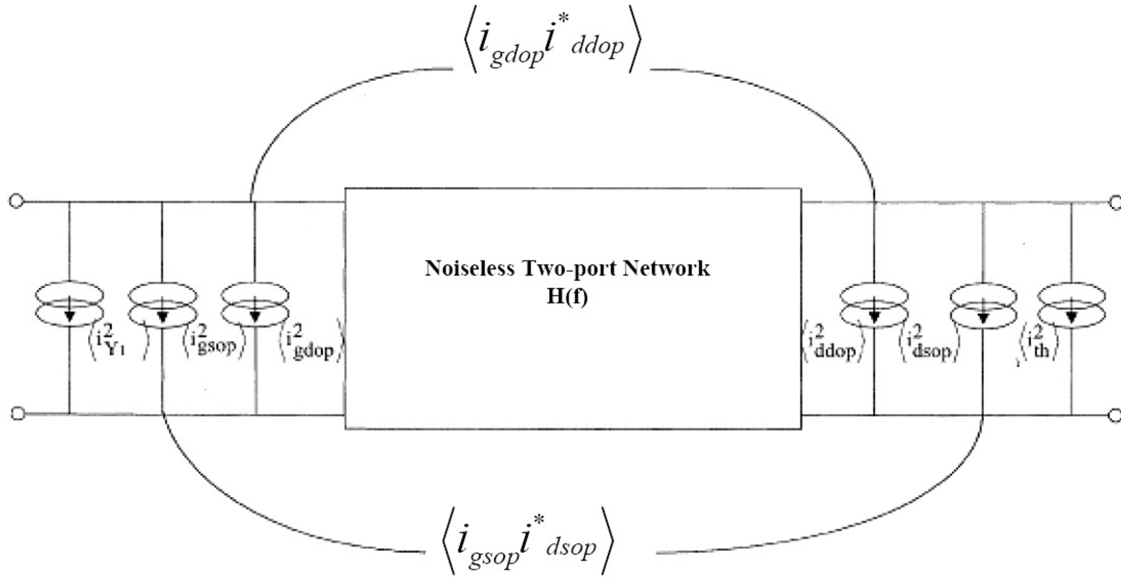

Fig.2. Noiseless two port network.

2.1. Diffusion noise components

The diffusion noise components arise from the random movements of the carriers (including those generated by the absorption of including radiation) in the channel due to thermal interaction between the free carriers and vibration ions. A noisy MISFET photodetector with a leaky gate can be represented by noiseless two port device (Fig. 2.) associated with the following noise sources.

(i) Diffusion noise has two components e.g., gate induced diffusion noise $\langle i^2_{gdop} \rangle$, drain diffusion noise $\langle i^2_{ddop} \rangle$ at the output.

(ii) The correlated diffusion noise sources e.g., the gate diffusion noise current source in the illuminated condition and the drain diffusion noise current in the illuminated condition. These components result from the spontaneous fluctuations due to thermal interactions between thermally as well as optically generated excess carriers under vibrating ions in the channel. At high frequency, the diffusion noise sources can be represented by two current generators i_{gdop}, the gate diffusion noise current in the illuminated condition and i_{ddop}, the drain diffusion noise current in the illuminated condition. These components are the short circuited noise currents at the input and output respectively when both input and output are short circuited. i_{gdop} will have a component that is partially correlated with i_{ddop}. This is due to the fact that the distributed noise e.m.f in the channel develops noise voltage along the channel in addition to the noise current i_{ddop} through the short circuited output. Due to capacitive coupling between the channel and the gate, these noise voltages circulate a capacitive noise current through the short circuit input. Hence the component i_{gdop} and i_{ddop} will be partially correlated. When the MESFET works in the photodetector mode the diffusion current component as well as the correlated components is greatly influenced by the received optical signal through photoconductive and photovoltaic effects.

Under the optically controlled condition, the diffusion noise component of the MISFET both at the drain end and at the gate end can be written as

$$\langle i^2_{ddop} \rangle = 4kTg_{mop}\Delta f P' \tag{1}$$

$$\langle i^2_{gdop} \rangle = \frac{4kT\Delta f}{g_{mop}} \omega^2 C^2_{gsop} R' \tag{2}$$

$$\langle ig_{dop} i^*_{ddop} \rangle = j4kT\Delta f \omega C_{gsop} Q' \tag{3}$$

where, k is Boltzmann's constant, T is the absolute temperature, ω is the angular frequency of the modulation signal, Δf is the bandwidth, and g_{mop} is the transconductance of the MISFET in the illumination condition.

The are MISFET bias dependent parameters P', Q' and R' are given by

$$P' = \frac{h_1(V_{gs}, V_{ds}, V_{op})}{\left[1-\left(\frac{V_{gs}-V_{op}}{V_p}\right)^{\frac{1}{2}}\right] f_1(V_{gs}, V_{ds}, V_{op})} \quad (4)$$

$$Q' = \frac{g_2(V_{gs}, V_{ds}, V_{op})}{f_1^2(V_{gs}, V_{ds}, V_{op}) f_2(V_{gs}, V_{ds}, V_{op})} \quad (5)$$

$$R' = \frac{g_3(V_{gs}, V_{ds}, V_{op})\left[1-\left[V_{gs}-V_{op}\right]^{\frac{1}{2}}\right]}{f_1^2(V_{gs}, V_{ds}, V_{op}) f_2^2(V_{gs}, V_{ds}, V_{op})} \quad (6)$$

Here g_2, g_3 and f_1,f_2, are the function of V_{gs} the gate-to-source voltage, V_{ds} the drain-to-source voltage, V_{op} the photovoltage developed at the Schottky gate contact under illuminated condition and V_p is the pinch-off voltage. The functions f_1 and f_2 have been obtained as

$$f_1(V_{gs}, V_{ds}, V_{op}) = \left[\left(\frac{V_{gs}-V_{ds}-V_{op}}{V_p}\right) - \left(\frac{V_{gs}-V_{op}}{V_p}\right)\right] - \frac{2}{3}\left[\left(\frac{V_{gs}-V_{ds}-V_{op}}{V_p}\right)^{\frac{3}{2}} - \left(\frac{V_{gs}-V_{op}}{V_p}\right)^{\frac{3}{2}}\right] \quad (7)$$

$$f_2(V_{gs}, V_{ds}, V_{op}) = \frac{\left\{\frac{2}{3}\left[\left(\frac{V_{gs}-V_{ds}-V_{op}}{V_p}\right)^{\frac{3}{2}} - \left(\frac{V_{gs}-V_{op}}{V_p}\right)^{\frac{3}{2}}\right] - \frac{1}{2}\left[\left(\frac{V_{gs}-V_{ds}-V_{op}}{V_p}\right)^{2} - \left(\frac{V_{gs}-V_{op}}{V_p}\right)^{2}\right]\right\}\left[1-\left(\frac{V_{gs}-V_{op}}{V_p}\right)^{\frac{1}{2}}\right]}{\left[f_1(V_{gs}, V_{ds}, V_{op})\right]^2} - \frac{\left\{\left(\frac{V_{gs}-V_{op}}{V_p}\right)^{\frac{1}{2}} - \left(\frac{V_{gs}-V_{op}}{V_p}\right)\right\}}{f_1(V_{gs}, V_{ds}, V_{op})} \quad (8)$$

The functions g_2 and g_3 are given by

$$g_2(V_{gs}, V_{ds}, V_{op}) = p(V_{gs}, V_{ds}, V_{op}) h_1(V_{gs}, V_{ds}, Vop) - h_2(V_{gs}, V_{ds}, V_{op}) \quad (9)$$

$$g_3(V_{gs}, V_{ds}, V_{op}) = p^2(V_{gs}, V_{ds}, V_{op}) h_1(V_{gs}, V_{ds}, Vop) - 2p(V_{gs}, V_{ds}, V_{op}) h_2(V_{gs}, V_{ds}, V_{op}) + h_3(V_{gs}, V_{ds}, V_{op}) \quad (10)$$

where,

$$P(V_{gs}, V_{ds}, V_{op}) = \frac{-\frac{1}{3}\left[\left(\frac{V_{gs}-V_{ds}-V_{op}}{V_p}\right)^{\frac{3}{2}} - \left(\frac{V_{gs}-V_{op}}{V_p}\right)^{\frac{3}{2}}\left(\frac{V_{gs}-V_{ds}-V_{op}}{V_p}\right)^{\frac{3}{2}} - \left(\frac{V_{gs}-V_{op}}{V_p}\right)^{\frac{3}{2}}\right] + \frac{1}{6}\left[\left(\frac{V_{gs}-V_{ds}-V_{op}}{V_p}\right)^{2} - \left(\frac{V_{gs}-V_{op}}{V_p}\right)^{2}\right]}{f_1(V_{gs}, V_{ds}, V_{op})} + $$

$$+ \frac{\left[\left(\frac{V_{gs}-V_{op}}{V_p}\right) - \frac{2}{3}\left(\frac{V_{gs}-V_{op}}{V_p}\right)^{\frac{3}{2}}\right]\left[\left(\frac{V_{gs}-V_{ds}-V_{op}}{V_p}\right)^{\frac{1}{2}} - \left(\frac{V_{gs}-V_{op}}{V_p}\right)^{\frac{1}{2}}\right]}{f_1(V_{gs}, V_{ds}, V_{op})} + \left(\frac{V_{gs}-V_{ds}-V_{op}}{V_p}\right)^{\frac{1}{2}} \quad (11)$$

$$h_1(V_{gs}, V_{ds}, V_{op}) = \left[\left(\frac{V_{gs}-V_{ds}-V_{op}}{V_p}\right) - \left(\frac{V_{gs}-V_{op}}{V_p}\right)\right] + \frac{4}{3}\left[\left(\frac{V_{gs}-V_{ds}-V_{op}}{V_p}\right)^{\frac{3}{2}} - \left(\frac{V_{gs}-V_{op}}{V_p}\right)^{\frac{3}{2}}\right] + \frac{1}{2}\left[\left(\frac{V_{gs}-V_{ds}-V_{op}}{V_p}\right)^{2} - \left(\frac{V_{gs}-V_{op}}{V_p}\right)^{2}\right] \quad (12)$$

$$h_2(V_{gs}, V_{ds}, V_{op}) = \frac{2}{3}\left[\left(\frac{V_{gs}-V_{ds}-V_{op}}{V_p}\right)^{\frac{3}{2}} - \left(\frac{V_{gs}-V_{op}}{V_p}\right)^{\frac{3}{2}}\right] - \left[\left(\frac{V_{gs}-V_{ds}-V_{op}}{V_p}\right)^{2} - \left(\frac{V_{gs}-V_{op}}{V_p}\right)^{2}\right] + \frac{2}{5}\left[\left(\frac{V_{gs}-V_{ds}-V_{op}}{V_p}\right)^{\frac{5}{2}} - \left(\frac{V_{gs}-V_{op}}{V_p}\right)^{\frac{5}{2}}\right] \quad (13)$$

$$h_3(V_{gs}, V_{ds}, V_{op}) = \frac{1}{2}\left[\left(\frac{V_{gs}-V_{ds}-V_{op}}{V_p}\right)^2 - \left(\frac{V_{gs}-V_{op}}{V_p}\right)^2\right] - \frac{4}{5}\left[\left(\frac{V_{gs}-V_{ds}-V_{op}}{V_p}\right)^{\frac{5}{2}} - \left(\frac{V_{gs}-V_{op}}{V_p}\right)^{\frac{5}{2}}\right] + \left[\left(\frac{V_{gs}-V_{ds}-V_{op}}{V_p}\right)^3 - \left(\frac{V_{gs}-V_{op}}{V_p}\right)^3\right] \quad (14)$$

Further, f_1, f_2, g_2 and g_3 are basic dependent function of the MISFET, which also depend on the photo voltage developed at the Schottky barrier when the device is used under optically controlled condition. These functions can be obtained from the equations (4), (5) and (6) where V_{gsop} and V_{gdop} are the values of gate-to-source and gate-to-drain voltage in illumination condition, respectively. These are given in terms of gate-to-source voltage (V_{gs}), and photo voltage (V_{op}) as

$$V_{gsop} = -V_{gs} - V_{op} \quad (15)$$

$$V_{gdop} = -V_{gs} - V_{ds} - V_{op} \quad (16)$$

The photo voltage developed across the gated Schottky contact due to absorption of optical radiation in the channel region can as be obtained as

$$V_{op} = \frac{\eta kT}{q}\ln\left\{\frac{qG_{op}(y_{dgd} + y_{dgs})}{2Jsc}\right\} \quad (17)$$

where, η is the ideality factor, k is Boltzmann's constant, q is the electronic charge, y_{dgd} is the gate depletion width at drain end, y_{dgs} is the gate depletion width at source end and J_{sc} is the reverse saturation current density of the Schottky contact.

Here, G_{op} is the photo generation rate (per unit volume per unit time)

$$G_{op} = 2\frac{(1-R_m)(1-R_s)P_{opt}}{h\upsilon} \times \left\{\frac{1}{y_{dgs} + y_{dgd}} + \frac{\exp(-\alpha y_{dgd}) - \exp(-\alpha y_{dgs})}{\alpha(y^2{}_{dgd} - y^2{}_{dgs})}\right\} \quad (18)$$

where, R_m is the reflection coefficient at entrance, R_s is the reflection coefficient at the metal-semiconductor interface, p_{opt} is the incident optical power density, h is the Planck's constant, and υ is the frequency of the incident light.

2.2. Shot noise components

Shot noise is produced by the quantum nature of photons arriving at the detector and related detection statistics. The noise produced is related directly to the amount of light incident on the photodetector and is a function of average optical power. The shot noise current present at the output of the MISFET photodetector due to gate leakage current is i_{dsop}. The shot noise current present at the input of the MISFET photodetector due to gate leakage current is i_{gdop} and the correlated shot noise current sources arise from the gate leakage current of the MISFET in the illuminated condition. When the MISFET is used as the photodetector, the gate leakage current is significantly increased by the received optical signal. This results in an increase in shot noise current components. The shot noise current source due to gate leakage current is represented at the device input as i_{gdop}. It shall be noted that since the gate leakage current flows through the channel under the gate it also produces shot noise current source in the drain circuit which is denoted by $i_{dsop.}$

In the present analysis, the MISFET has been assumed to have a leaky gate. The shot-noise current component arises from the gate leakage current that flows in the gate current. This leakage current increases considerably in the presence of incident radiation. The gate leakage current also flows in the channel, which creates fluctuation drain current. This component constitutes the drain-shot-noise and gate-shot-noise component. Like the diffusion noise component, these two shot- noise components are also partially correlated. However, as the physical origin of the shot-noise and the diffusion-noise components are different, there is no correlation in between these components.

The gate-shot-noise component present at the input of the MISFET due to gate leakage current is given by

$$\left\langle i^{2q1}{}_{gsop}\right\rangle = 2qI_{Gop}(2\pi f) \quad (19)$$

where, I_{Gop} is the dc component of the gate leakage current under illuminated condition.

The gate leakage current under illuminated condition given by

$$I_{Gop} = I_{Gs} + I_{op} \quad (20)$$

The drain shot-noise current is given by

$$\left\langle i^2{}_{gsop}\right\rangle = \alpha qI_{Gop}(2\pi f) \quad (21)$$

where, α is the constant varying from 0.5 to 1.5 for MISFET. The noises current due to correlation between drain and gate shot-noise components can be written as

$$\left\langle i_{gsop} i^*{}_{dsop}\right\rangle = -\sqrt{2\alpha qI_{Gop}(2\pi f)} \quad (22)$$

As the physical origin of the diffusion-and the shot-noise components are different, the mean-square values of the

gate-noise, drain-noise, and these correlation-noise-current components can be written as

$$\left\langle i^2{}_{gop} \right\rangle = \left\langle i^2{}_{gdop} \right\rangle + \left\langle i^2{}_{gsop} \right\rangle \quad (23)$$

$$\left\langle i^2{}_{dop} \right\rangle = \left\langle i^2{}_{ddop} \right\rangle + \left\langle i^2{}_{dsop} \right\rangle \quad (24)$$

$$\left\langle i_{gop} i^*{}_{dop} \right\rangle = \left\langle i_{gdop} i^*{}_{ddop} \right\rangle + \left\langle i_{gsop} i^*{}_{dsop} \right\rangle \quad (25)$$

2.3. Thermal noise components

Thermal noise components are arising from the random motion of electrons in a conductor. It is often described by how much dB higher than the room-temperature lower limit of-174 dBm/Hz. To reduce the thermal noise, a low-noise amplifier can be connected after the photodiode. Typical noise figures for amplifiers range above -174dB/Hz for narrow-band amplifiers, 6 to 8 dB for low-noise, wider-band amplifiers and 15dB for high-frequency amplifiers. Therefore, there should be a trade off between sensitivity and bandwidth when choosing amplifiers. The noise increases as the bandwidth increases.

The thermal noise current sources arising from various bias resistances are the device intrinsic resistance and the input resistance of the following preamplifier. Thermal noise at input due to pad resistance R_L and gate-bias resistance R_{GG} are given by

$$\left\langle i^2 th \right\rangle = 4kT(2\pi f)\frac{1}{R_{eq}} \quad (26)$$

$$\frac{1}{R_{eq}} = \frac{1}{r_{dsop}} + \frac{1}{R_{DD}} + \frac{1}{R_i} \quad (27)$$

The thermal noise due to different resistive components at the output can be obtained as

$$\left\langle i^2{}_{th} \right\rangle = \frac{4kT\Delta f}{R_{eqop}} \quad (28)$$

where, Δf is the bandwidth, and R_{eqop} is the equivalent resistance at the output in the illumination condition, given by

$$\frac{1}{R_{eqop}} = \frac{1}{R_D} + \frac{1}{R_i} + \frac{1}{r_{dsop}} \quad (29)$$

where, R_D is the drain-bias resistance, R_i is the input resistance of the following stage, and r_{dsop} is the source-to-drain resistance in illumination condition.

2.4. Signal-to-noise ratio (SNR)

In order to compute the signal-to-noise ratio of the MISFET photodetector at the output side, we develop a high frequency equivalent model and is shown in Fig.3. It may be noted that although the individual diffusion noise sources and shot noise sources of the drain and gate are correlated, the diffusion and shot noise sources are not correlated since their physical origin is different. Therefore, the total gate and drain current sources and their cross correlation can be written as

$$\left\langle i_{gop}^2 \right\rangle = \left\langle i_{gdop}^2 \right\rangle + \left\langle i_{gsop}^2 \right\rangle \quad (30)$$

$$\left\langle i_{dop}^2 \right\rangle = \left\langle i_{ddop}^2 \right\rangle + \left\langle i_{dsop}^2 \right\rangle \quad (31)$$

$$\left\langle i_{gop} i_{ddop}^2 \right\rangle = \left\langle i_{gdop} i_{ddop}^* \right\rangle + \left\langle i_{gsop} i_{dsop}^* \right\rangle \quad (32)$$

where, $\left\langle i_{gop}^2 \right\rangle, \left\langle i_{dop}^2 \right\rangle$ are the overall mean square noise current of the gate and the drain respectively $\left\langle i_{gop} i_{ddop}^* \right\rangle$ is the overall mean square noise current of correlated components.

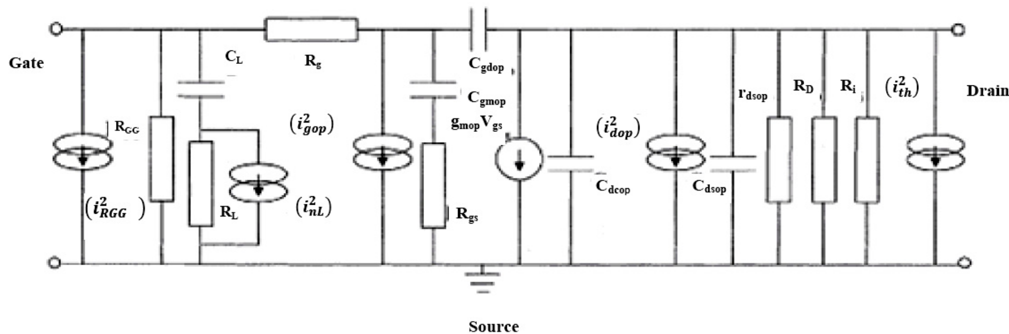

Fig. 3. High frequency equivalent model.

In the photodetector, the excess the electron-hole pairs generated in the gate depletion, substrate depletion region and the neutral channel region result in the development of internal and external photo voltages and the gate-channel and substrate- channel barriers respectively. The photovoltages together with the change in conductance of the channel give rise to a change in the various current components of the device. This results in the changes in the various device parameters such as gate-to-source capacitance (C_{gs}), channel capacitance (C_{dc}), transconductance g_{mop} and the drain-to-source resistance r_{dsop} etc. Therefore, when the MISFET is used as the photodetector, the effects of the received light on these parameters are to be carefully considered for noise modeling of the device. The diffusion noise component of the gate is influenced by the received optical signal through a change in the gate-to-source capacitance as well as the transconductance of the device in the illuminated condition. This component is also affected by the forward photovoltage generated by the received optical signal. The noise component of the gate is also affected by the excess electron-hole pairs generated by the received optical signal just below the gate. The diffusion noise component on the drain side is only affected by change in the transconductance of the device and the photovoltage in the illuminated condition. The GLC has the similar effect in the illuminated condition as discussed before.The cross correlation between the gate and drain noise sources is influenced by gate-to-source capacitance and the photovoltage in the illuminated condition.

The output signal-to-noise ratio (SNR) in the illuminated condition is an important parameter for characterization of the MISFET. In order to calculate the SNR at the output, the noise equivalent circuit of the MISFET is represented by a noiseless two-port network along with various noise-current sources, as shown Fig. 2.For calculation of the transfer function of the two-port network, the high –frequency noise equivalent circuit of the MISFET is first transformed into Thevenin's equivalent circuit. The voltage gain of the two-port network is given by

$$A_v = \frac{V_o}{V_{gs}} = \frac{I_{sh}Z}{V_{gs}} \quad (33)$$

where, I_{sh} is the short circuited current at the output and V_{gs} is the input voltage across c_{gs}. It is seen that Z is the parallel combination of impedances corresponding to R_D, R_i, r_{dsop}, c_{ds} and c_{gs}.

The input admittance can be expressed as

$$Y = \frac{1}{Z} = \frac{1}{R_{eq}} + j2\pi f(C_{dcop} + C_{dsop} + C_{gdop}) \quad (34)$$

Here C_{dop} is the channel capacitance, C_{dsop} is the drain-to-source capacitance, and C_{gdop} is the gate-to-drain capacitance.

The current in the direction from drain to source in a zero resistance wire connecting the output terminal is given by

$$I = -g_{mop}V_{gs} + (j2\pi f C_{gdop})V_{gs} \quad (35)$$

$$|A_v| = \frac{-g_{mop} + j2\pi f c_{gdop}}{\frac{1}{R_{eq}} + j2\pi f\left(c_{gdop} + c_{dsop} + c_{dcop}\right)} \quad (36)$$

$$Y_i(f) = j2\pi f C_{gsop} + (1 - A_v)j2\pi f C_{gdop} + \frac{1}{R_{GG}} \quad (37)$$

Here, R_{GG} is the gate-bias resistance, and $|A_v|$ is the magnitude of the voltage gain of the two-port network.

The transfer function of the two-port network is given by

$$H(f) = \frac{g_{mop}}{j2\pi f C_{gsop} + (1 - A_v)j2\pi f C_{gdop} + \frac{1}{R_{GG}}} \quad (38)$$

When the MISFET is operated as an optically controlled device, no physical ac signal is present between the gate and the source. The photovoltage developed at the Schottky gate contact in the illumination condition has been mapped as the signal voltage in the present analysis and the photovoltage in the gate circuit that drives the signal current in the input.

This can be represented by the signal source given by

$$i_{signal} = \frac{V_{op}}{R_{gg}} \quad (39)$$

where, V_{op} is the photovoltage across the Schottky gate.

The output signal power, S can be obtained at the output side as

$$S = i_{signal}^2 * |H(f)|^2 \quad (40)$$

The output noise powering can be written as

$$N = \langle i_{gop}^2 \rangle |H(f)|^2 + \langle i_{gop} i_{dop}^* \rangle |H(f)| + \langle i_{dop}^2 \rangle + \langle i_{th}^2 \rangle R_{eq} \quad (41)$$

Therefore the signal-to-noise ratio can be obtained as

$$SNR = \frac{i_{signal}^2 * |H(f)|}{\langle i_{gop}^2 \rangle |H(f)|^2 + \langle i_{gop} i_{dop}^* \rangle |H(f)| + \langle i_{dop}^2 \rangle + \langle i_{th}^2 \rangle R_{eq}} \quad (42)$$

2.5. Bit error rate (BER)

Among a group of optical receivers, a receiver is said to more sensitive if it achieves the same performance with less optical power incident it. The performance criterion for digital receiver is governed by BER defined as the

probability of incorrect identification of a bit by the decision circuit of a receiver. Hence BER of 2x10^{-6} corresponds to an average 2 errors per million bits. A commonly used criterion for digital optical receiver required the BER to a below 1x10^{-9}. This is calculated by the formula

$$BER = \frac{1}{\sqrt{2\pi}\ Q}\exp\left(-\frac{Q^2}{2}\right) \quad (43)$$

2.6. Noise equivalent power (NEP)

An important parameter which describes the noise performance of a photodetector is the noise equivalent power (NEP). The sensitivity of a photodetector is an important characteristic and is defined as the minimum optical input power needed to achieve a signal-to-noise ratio greater than a given value. A convenient measure of sensitivity is the noise equivalent power. Thus, when the rms signal power is equal to noise equivalent power, the photocurrent is equal to the noise current and the signal-to-noise ratio is unity. The noise equivalent power is calculated for bandwidth B=1Hz.

$$NEP = \frac{h\nu}{q\eta}\left(2q\left(I_{ph} + I_B + I_D\right) + \frac{4k_BT}{R_{eq}}\right) \quad (44)$$

From the equation (44), it is clear that to increase the sensitivity of the photodetector,n and R_{eq} should be as large as possible, and the unwanted currents I_B and I_D should be as small as possible.Thus, the noise equivalent power is a measure of minimum detectable power.

3. Results and discussion

The 3D Poisson's equation is solved using Liebmann's iterative method to determine the surface potential at illuminated and dark conditions for a fixed value of gate voltage and assumed value of the drain voltage. The numerically estimated value of the surface potential is utilized to determine the electric field and mobility in all the three directions. The drain current has been calculated. The voltage profile and the electric field distribution in the channel have been estimated for accurate calculation of the drain to source current. The voltage profile in the channel is obtained by calculating the differential change in the voltage across the channel and is assumed to be very small at the source end and low field mobility has been used to begin the numerical computation from the source end.

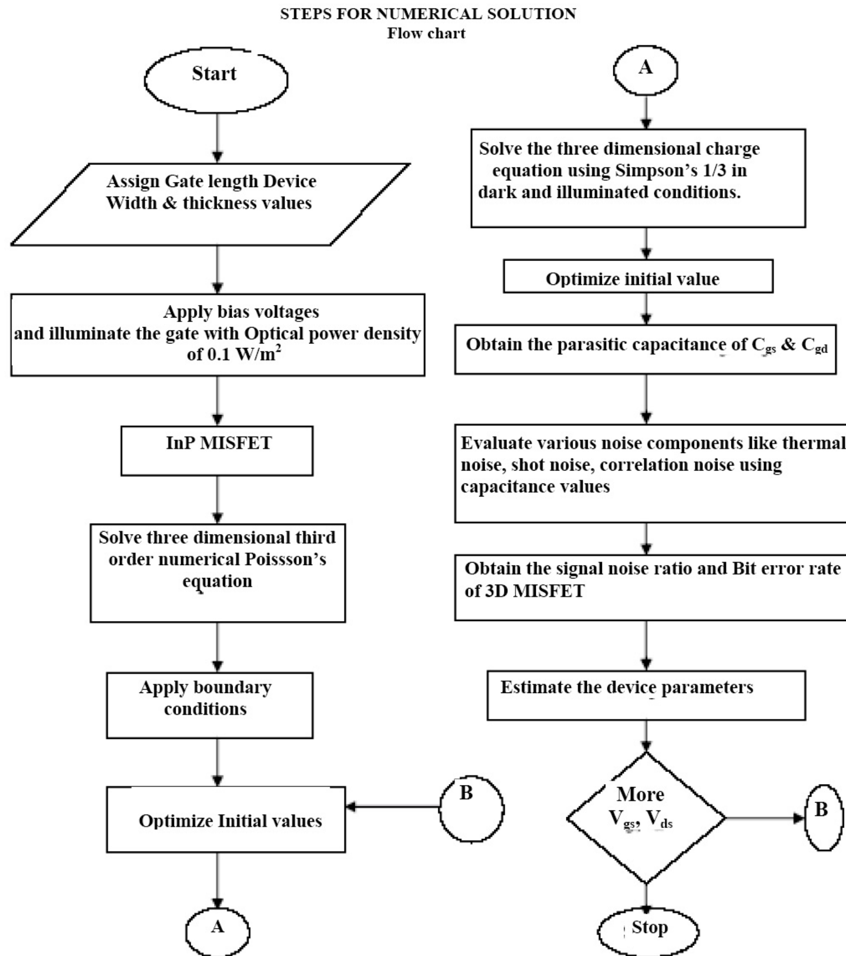

Fig.4.Flowchart represents the numerical noise simulation of MISFET photodetector

The steps for numerical solution for the computation of device parameters and noise components of the MISFET photodetector is described as a flow chart and it is given in Fig.4.

Computations have been carried out for the InP MISFET photodetector under dark and illuminated conditions to check its use as a high speed photo detector.

Table.2. Parameters and value used for numerical modeling.

Parameter	Value
Gate Length	100 nm
Device width	80 nm
Oxide layer thickness	30 nm
Absorption coefficient(α)	10^6/m
Intrinsic carrier concentration(n_i)	$1.2x10^{13}/m^3$
Acceptor concentration(N_a)	$10^{21}/ m^3$
Critical field(E_c)	$1.65×10^6$V/ m
Low field mobility($μ_o$)	$0.2m^2$/V .s
Capacitance	$3 × 10^8$ F/m^2
Energy gap at 300K	1.12 eV
Temperature(T)	300 K
Low field mobility($μ_0$)	0.2 m^2/V.s

The variation of shot noise componets with frequency is depicted in Fig. 5. When the MISFET is used as a photodetector the gate leakage current is significantly increased by the received optical signal. This results in an increase shot noise current components. The total noise component increases faster with frequency as compared to the correlation noise components. It is seen that the total noise power delivered at the output remains almost constant at lower frequency and decreases with increase in frequency. This may be due the fact that the magnitude of the transfer function of the two port network decreases with increase in frequency. So, the contribution of the input noise components to the output decreases with increase in frequency. The total noise power is dependent on the incident optical power at a particular frequency. It is also seen that the total noise power due to various noise components at the output is independent of the incident optical power.

Fig. 6. shows the variation of the signal-to-noise ratio at the output of the MISFET photodetector with operating frequency for various values of feed back resistors. It is seen that for given optical power of signal to noise ratio remains constant for low values of resistance. As the value of resistance increases the signal to noise ratio increases. The increase in signal to noise ratio at higher frequency is attributed to the increase in the various noise components at higher frequencies.

The parameters used for the calculations are given in Table 2. Calculations have been carried out for an InP/ Al_2O_3 MISFET configuration with a semi-transparent metal gate. The effects of illumination on the gate terminal of the device have also been considered.

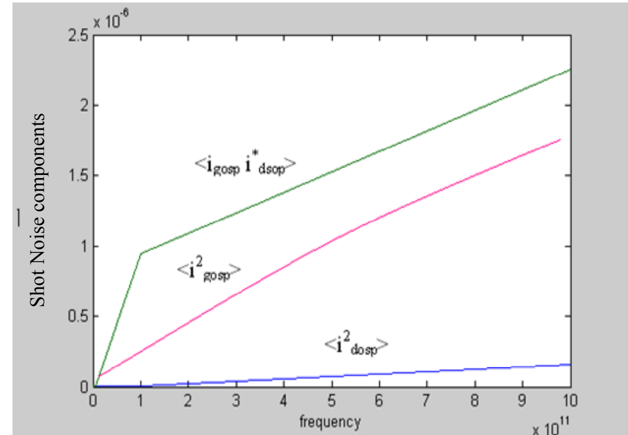

Fig.5. Variation of shot noise components with operative frequencies.

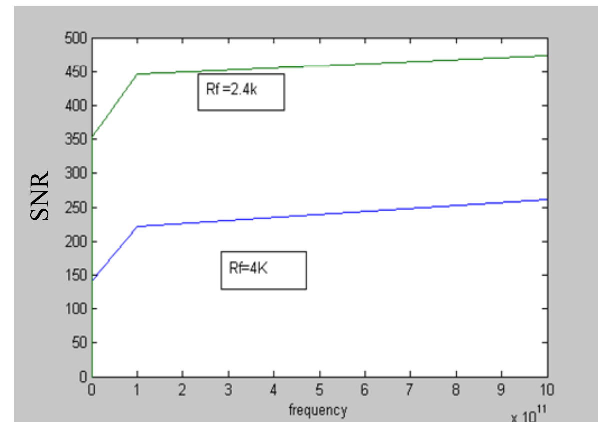

Fig.6. Variation of signal-noise ratio with frequency for various values of resistances.

Fig. 7 shows the variation of bit error rate of the MISFET with frequency. It is seen that the bit error rate increases as the frequency increases. For any digital communication system application the bit error rate is an important parameter and it depends on the signal to noise ratio of the detector. It is also seen that the device has the bit error rate of 5.5x 10^{-9} at the optimum gain. This is well above the acceptable value of bit error rate of 10^{-9} for photo detector presently used in optical communication system. However, the BER and the receiver sensitivity, depend on the modulation format as well as on the demodulation scheme used by the coherent receiver.

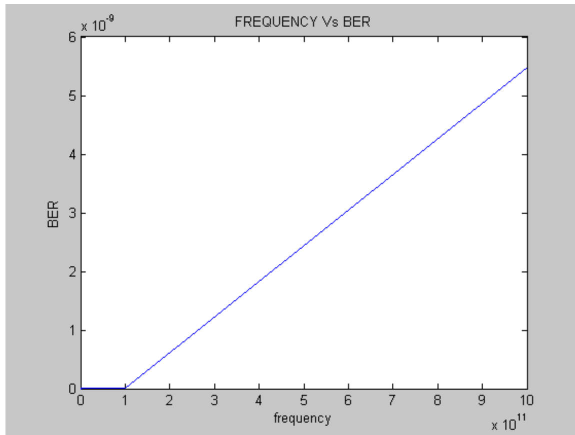

Fig.7. Variation of BER with frequency

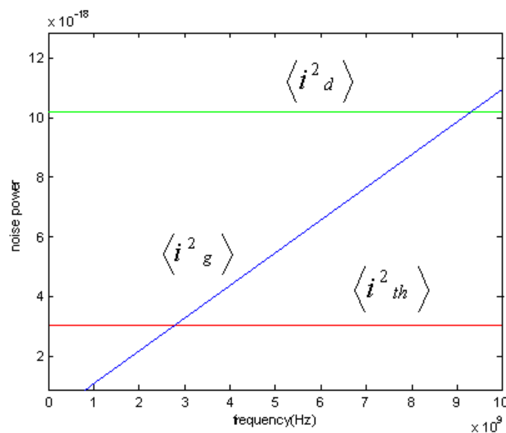

Fig. 8 Variation of various noise components with frequency.

Fig. 8 shows the variation of different noise components with frequency. It is seen that the mean square value of total gate-noise components and total drain-noise components are constant. It is also seen that the thermal noise components are constant and independent of frequency have relatively higher values as compared with the gate noise components. Some of the noise components occur between the gate input and the source input and others appear directly across the output terminals. The input noise components are transferred to the output for the computation of the total noise power delivered at the output. The magnitude of the transfer function is used for the transferring the input noise component into the output.

Fig.9. shows the variation of noise equivalent power (NEP) of the MISFET with frequency for different values of gate leakage current (I_{GS}). An important parameter of an optical detector is the noise equivalent power. It is seen that the noise equivalent power is almost constant up to few gigahertz and it increases rapidly with increase in frequency. This is due to the fact that an increase in the current causes increase in shot noise current component and a decrease in the gate voltage. This larger noise with increase in current calls for a larger signal power to match the noise at the receiver output.

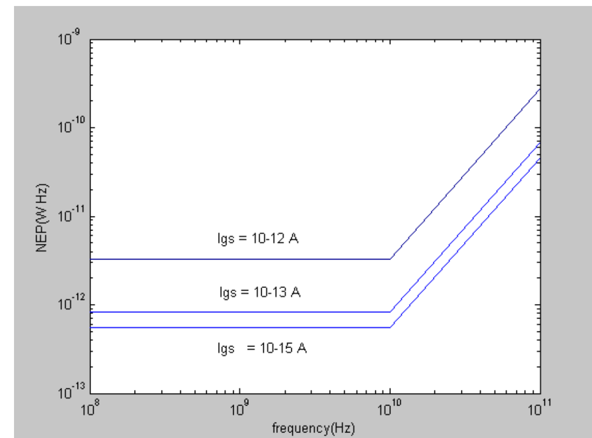

Fig. 9 Variation of noise equivalent power (NEP) with frequency.

4. Conclusions

The noise model presented here can be used for the theoretical characterization of optically gated three dimensional MISFET as a photodetector. The noise behavior of the MISFET has been studied theoretically. The noise characteristics depend on the value of incident optical power. The results that are obtained show that the photogenerated carriers enhance the gate leakage current and degrade the noise performance of MISFETs under optically controlled condition. This reveals that the operating frequency can be adjusted suitably to make the noise behavior. In conclusion, the device can be used as photodetector in OEIC receivers.

Acknowledgements

The authors are grateful to the All India council for Technical Education (AICTE), New Delhi, India for providing research grants (0023/BOR/RPS/080/06/07) in the year 2006-2007.

References

[1] S.M. Sze, "Physics of semiconductor Devices", 2nd Edition, Wiley Eastern Ltd., New Delhi, India (1981).
[2] E. Yamaghuchi, T. Kobayashi, "Optically-gated InP MISFET: A New high-gain optical detector," Japan J. Appl. Physics, **21**, 104 (1975).
[3] P. Chakrabarti, S. Kumar, P.K. Rout, B.G. Rappai, "A proposed MISFET photodetector," Proc. 3rd Asia Pacific Microwave Conf., Tokyo, Japan, 575 (1990).

[4] P. Chakrabarti, I. Venugopal, "Charge-sheet model of a proposed MISFET photodetector," Phys. Stat. Sol.(a), **128**, 521 (1991).
[5] K. Ohata, "InP MISFET", Workshop Dig., Asia Pacific Microwave Conference, Tokyo, Japan, 15 (1990).
[6] M. Kabeer, K. Gowri, V. Rajamani, "Three Dimensional Modeling and Simulation of a Nano MISFET Photodetector", J. Optoelectron. Adv. Mater., **9**(9), 2879 (2007).
[7] Saman Asgaran, M.Jamal Deen, "Analytical modeling of MOSFET's channel noise and noise parameters", IEEE Transactions on Electron devices, **51**(12), 2109 (2004).
[8] Mini Nanua, David Blaauw, "Noise analysis methodology for partially Depleted SOI circuits", IEEE Transactions on Solid state circuits, **39**(9), 1581 (2004).
[9] K. T. Yan, Leonard Forbes," l/f Bulk phenomena noise theory for GaAs MESFETs" IEEE, Microelectronics and VLSI.1995, TENCON'95, 111 (1999).
[10] Olivera Pronic , Vera Markovie ." A wave approach to signal *and n*oise modeling of dual-gate MESFET " Radar and wireless communication , 287 (2005).
[11] N. Males-IliC, V. Markovic, B. Milovanovid ," New MESFET Noise Models as User-Defined elements of Program Libra Library", Microelecronics 2000 proceedings, 137 (2000).
[12] Chih-Hung Chen, M. Jamal Deen, "Channel Noise Modeling of Deep Submicron MOSFETs", IEEE Trans Electron Devices, **49**(8), 1484 (2002).
[13] Z.Celik-Butler, "Low- frequency noise in deep-submicron metal-oxide-semiconductor field -effect transistor", IEE Proc-Circuits,Devices and Systems , **149**(1), 23 (2002).
[14] Jonghwan Lee, Gijs Bosman,, Keith R. Green, D. Ladwig," Noise Model of Gate-Leakage Current in Ultrathin Oxide MOSFETs", IEEE Trans. Electron Devices, **50**(12), 2499 (2003).
[15] M. Rudolph, R. Doerner, P. Heymann, L. Klapproth, G. Bock, "Direct Extraction of FET Noise Models From Noise Figure Measurements", IEEE Trans. Microwave Theory and Techniques, **50**(2), 461 (2002).
[16] Gholamreza Moradi, Abdolali Abdipour, "A simplified noise modeling of MM-wave FETs", Third International Conference on Millimeter wave Technology Proceedings, 312 (2002).

*Corresponding author: rajavmani@gmail.com, rajavmani@rediffmail.com